Inorganic Chemistry

Article

pubs.acs.org/IC

BTBPs versus BTPhens: Some Reasons for Their Differences in Properties Concerning the Partitioning of Minor Actinides and the Advantages of BTPhens

Frank W. Lewis,*[,†,⊥] Laurence M. Harwood,*[,†] Michael J. Hudson,[†] Michael G. B. Drew,[†] Véronique Hubscher-Bruder,[‡] Vladimira Videva,[‡] Françoise Arnaud-Neu,[‡] Karel Stamberg,[§] and Shyam Vyas[∥,#]

[†]Department of Chemistry, University of Reading, Whiteknights, Reading RG6 6AD, United Kingdom

[‡]Université de Strasbourg, IPHC, 25 rue Becquerel 67087 Strasbourg, France CNRS, UMR7178, 67037 Strasbourg, France

[§]Department of Nuclear Chemistry, Czech Technical University in Prague, Břehová 7, 11519 Prague 1, Czech Republic

[∥]National Nuclear Laboratory, Chadwick House, Warrington Road, Warrington WA3 6AE, United Kingdom

Supporting Information

ABSTRACT: Two members of the tetradentate *N*-donor ligand families 6,6′-bis(1,2,4-triazin-3-yl)-2,2′-bipyridine (BTBP) and 2,9-bis(1,2,4-triazin-3-yl)-1,10-phenanthroline (BTPhen) currently being developed for separating actinides from lanthanides have been studied. It has been confirmed that $CyMe_4$-BTPhen **2** has faster complexation kinetics than $CyMe_4$-BTBP **1**. The values for the HOMO−LUMO gap of **2** are comparable with those of $CyMe_4$-BTBP **1** for which the HOMO−LUMO gap was previously calculated to be 2.13 eV. The displacement of BTBP from its bis-lanthanum(III) complex by BTPhen was observed by NMR, and constitutes the only direct evidence for the greater thermodynamic stability of the complexes of BTPhen. NMR competition experiments suggest the following order of bis-complex stability: 1:2 bis-BTPhen complex ≥ heteroleptic BTBP/BTPhen 1:2 bis-complex > 1:2 bis-BTBP complex. Kinetics studies on some bis-triazine *N*-donor ligands using the stopped-flow technique showed a clear relationship between the rates of metal ion complexation and the degree to which the ligand is preorganized for metal binding. The BTBPs must overcome a significant (ca. 12 kcal mol^{-1}) energy barrier to rotation about the central biaryl C−C axis in order to achieve the *cis*−*cis* conformation that is required to form a complex, whereas the *cis*−*cis* conformation is fixed in the BTPhens. Complexation thermodynamics and kinetics studies in acetonitrile show subtle differences between the thermodynamic stabilities of the complexes formed, with similar stability constants being found for both ligands. The first crystal structure of a 1:1 complex of $CyMe_4$-BTPhen **2** with $Y(NO_3)_3$ is also reported. The metal ion is 10-coordinate being bonded to the tetradentate ligand **2** and three bidentate nitrate ions. The tetradentate ligand is nearly planar with angles between consecutive rings of 16.4(2)°, 6.4(2)°, 9.7(2)°, respectively.

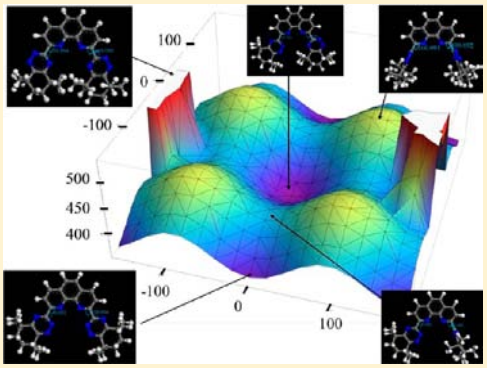

INTRODUCTION

In recent decades, much research has been carried out aimed at reducing the environmental impact of the spent fuel generated by nuclear power plants. This goal is becoming increasingly important as many countries consider expanding their civil nuclear power programs to meet future energy demands.[1] Although the PUREX process is currently used[2] to recover uranium and plutonium from used nuclear fuel, the remaining spent fuel still contains the minor actinides americium, neptunium, and curium which account for much of its long-term radiotoxicity. One strategy currently being pursued is "Partitioning and Transmutation",[3] whereby the radioactive minor actinides americium(III) and curium(III) are first separated from the nonradioactive lanthanides using a selective solvent extraction process (SANEX process),[4] and then converted into less radiotoxic elements by neutron-induced fission. This separation is necessary since the lanthanides have higher neutron capture cross sectional areas than the actinides and will thus absorb neutrons, which are required in the transmutation process, in preference to the actinides.[5]

Despite the chemical similarities between the two groups of elements,[6] soft N- and S-donor ligands have been shown to be capable of discriminating between the trivalent actinides (An(III)) and trivalent lanthanides (Ln(III)). The development of actinide-selective organic ligands has been the subject of several recent reviews.[7] The terdentate 2,6-bis(1,2,4-triazin-3-yl)pyridine (BTP)[8] and quadridentate 6,6′-bis(1,2,4-triazin-3-yl)-2,2′-bipyridine (BTBP)[9] ligands have so far shown the most promising properties for these separations in liquid−liquid

Received: December 6, 2012
Published: April 24, 2013

 © 2013 American Chemical Society dx.doi.org/10.1021/ic3026842 | *Inorg. Chem.* 2013, 52, 4993−5005

extraction tests. It has been demonstrated on genuine waste solution that $CyMe_4$-BTBP **1** (Figure 1) is a suitable ligand for

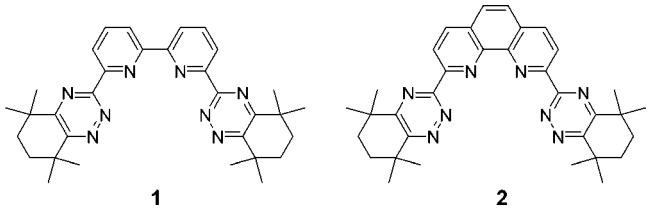

Figure 1. Structures of the ligands $CyMe_4$-BTBP **1** and $CyMe_4$-BTPhen **2**.

the separation of An(III) from Ln(III) in a laboratory-scale SANEX process, although a phase-transfer agent was needed to improve the otherwise slow extraction kinetics.[10] In addition, **1** is employed as the principal extractant in processes currently being developed for the selective extraction of actinides directly from PUREX raffinate.[11]

The ligand $CyMe_4$-BTPhen **2** (Figure 1) was recently reported as a promising candidate for the separation of actinides from lanthanides in the SANEX process.[12] This ligand has specific differences from the BTBPs. $CyMe_4$-BTPhen **2** is held in the *cis*−*cis* conformation and is thus more preorganized for complex formation; it has a dipole moment and is surface active at the interface.[13] Consequently, $CyMe_4$-BTPhen **2** shows faster rates of metal ion extraction and stripping together with distribution ratios which are 2 orders of magnitude higher for An(III) extraction in liquid−liquid extraction experiments than its non-pre-organized BTBP counterpart **1**. The improved kinetics of metal ion extraction by **2** compared to **1** can be attributed, at least in part, to higher concentrations of the ligand **2** at the phase interface. Some additional examples of 2,9-bis-(1,2,4-triazin-3-yl)-1,10-phenanthroline (BTPhen) ligands were reported recently.[14] However, although the underlying reasons for the higher extraction capabilities exhibited by the BTPhen ligands (and **2** in particular) are beginning to be understood, a basic knowledge of the thermodynamics and kinetics of the interactions of actinide and lanthanide cations with bis-triazine N-donor ligands is nevertheless essential to better understand the coordination chemistry of the ligands that will eventually be chosen for use in the SANEX separation process.

Quantum mechanics calculations suggest that BTPhens are more basic than BTBPs and form more stable complexes with Eu(III).[15] In addition, it has been shown that increasing the degree of ligand preorganization within a series of polypyridine ligands leads to progressively greater complex thermodynamic stabilities with a variety of metal ions.[16] For example, the preorganized ligands 2,9-di(2-pyridyl)-1,10-phenanthroline (which is closely related to **2**)[17] and 2-(pyrid-2′-yl)-1,10-phenanthroline[18] form lanthanide(III) complexes with larger stability constants than their non-pre-organized analogues 2,2′:6′,2″:6″,2‴-quaterpyridine and 2,2′:6′,2″-terpyridine, respectively. On the other hand, recent investigations in solution and in the solid state show no significant differences in the speciation of **1** and **2** with trivalent lanthanide nitrates,[19] and show that 1:2 complexes with comparable thermodynamic stabilities are the major species formed under extraction relevant conditions.[19,20] Thermodynamic and kinetic parameters for the complexation of some BTP and BTBP ligands (including $CyMe_4$-BTBP **1**) with some Ln(III) cations in homogeneous medium were also previously reported.[21]

In order to gain further insights into the reasons for the differences in extraction properties between BTPhens and BTBPs, we report herein the results of our investigations using detailed molecular modeling calculations,[22,23] lanthanide NMR titrations and competition experiments, thermodynamic and kinetic studies in solution, and X-ray crystallography. An analysis of the conformations of ligands **1** and **2** has been carried out using DFT calculations. The thermodynamics and kinetics of complex formation between $CyMe_4$-BTPhen **2** and some representative Ln(III) cations and Y(III) were then studied by spectrophotometry and microcalorimetry under conditions identical to those reported previously.[21] Finally, the complexation of **1** and **2** with selected lanthanides has been investigated by NMR spectroscopic titrations and lanthanide binding competition experiments.

EXPERIMENTAL SECTION

Molecular Modeling Calculations. The conformational space of ligands **1** and **2** was searched using a systematic approach by varying specific torsion (rotational) angles in sequence, rather than by using a Monte Carlo approach. The conformer analysis tools within the Materials Studio software package[24] were used to carry out the simulations. These tools vary the selected angles within the molecule in user defined steps and calculate the energy at each point, so generating a conformational map of the most likely states the molecule will occupy. In some cases this approach may generate highly strained structures that are unrealistic. These are briefly optimized using the density functional code, DMol within the Materials Studio software package.[25] This code removes the close contacts and allows bond lengths in the molecule to change, but will keep the molecule in the same conformation. In the case of ligand **1**, the three torsion angles (the triazine−pyridine, pyridine−pyridine, and pyridine−triazine dihedral angles) were varied systematically in steps of 30° generating a total of 1722 conformers (after the duplicates are removed). These were subsequently optimized using the DMol code using the COARSE setting (which sets the tolerances for parameters such as the optimizer, number of SCF cycles, exact details are in the Supporting Information) and the BLYP functional. In the case of ligand **2**, the two torsion angles (the two triazine−phenanthroline dihedral angles) were varied systematically in steps of 10° generating a total of 324 conformers. The energies of the conformers were calculated using the COMPASS forcefield.[26] For ligand **2**, the two lowest energy conformations were further optimized using DFT to calculate more accurate energy differences. A full description of the settings used in these calculations can be found in the Supporting Information.

Materials. The ligands $CyMe_4$-BTBP **1**[27] and $CyMe_4$-BTPhen **2**[12] (Figure 1) were synthesized as described previously. The aliphatic diketone precursor to ligands **1** and **2** was synthesized by a new procedure.[28] Methanol-Chromasolv (Sigma-Aldrich, maximum 0.03% water) and acetonitrile (Riedel-deHaën, maximum 0.1% water) were used without any further purification. The supporting electrolyte Et_4NNO_3 (Acros, 99%) was dried under vacuum for 24 h at room temperature. The following metal salts were used for the spectrophotometric and microcalorimetric titrations: $La(NO_3)_3{\cdot}6H_2O$, $Eu(NO_3)_3{\cdot}H_2O$, $Yb(NO_3)_3{\cdot}xH_2O$, and $Y(NO_3)_3{\cdot}xH_2O$ (Alfa Aesar, 99.99%). These salts were dried under vacuum before use, and stock solutions of all of them were standardized by complexometric titrations with EDTA.[29] The following metal salts were used for the NMR titrations: $La(NO_3)_3{\cdot}6H_2O$, $Lu(NO_3)_3{\cdot}6H_2O$, $Eu(NO_3)_3{\cdot}5H_2O$, $Ce(NO_3)_3{\cdot}6H_2O$, and $Y(NO_3)_3{\cdot}6H_2O$ (Aldrich).

X-ray Crystallography. Independent reflection data (11 458) were collected with Mo Kα radiation at 150 K using the Oxford Diffraction X-Calibur CCD System. The crystal was positioned at 50 mm from the CCD, and 321 frames were measured with counting times of 10 s. Data analysis was carried out with the CrysAlis program.[30] The structure was solved using direct methods with the

dx.doi.org/10.1021/ic3026842 | Inorg. Chem. 2013, 52, 4993−5005

SHELXS97 program.[31] The non-hydrogen atoms were refined with anisotropic thermal parameters. The hydrogen atoms bonded to carbon were included in geometric positions and given thermal parameters equivalent to 1.2 times (or 1.5 times for methyl groups) those of the atom to which they were attached. Absorption corrections were carried out using the ABSPACK program.[32] The structure was refined using SHELXL97[31] on F^2 to R1 0.0680, wR2 0.1336 for 7649 data with $I > 2\sigma(I)$.

Spectrophotometric Study. The overall stability constants β, equal to the molar ratio $[M_xL_y^{xn+}]/[M^{n+}]^x[L]^y$ (M^{n+} = cation, L = ligand), were determined by UV absorption spectrophotometry at 25.0 ± 0.1 °C in methanol and in acetonitrile. The constant ionic strength was provided by 10^{-2} M Et_4NNO_3. Suprasil quartz cells of 1 cm path length were used. The spectral changes of 2.5 mL of solutions of ligand **2** upon stepwise additions (10 μL) of metal nitrate solution directly into the measurement cell were recorded from 250 to 400 nm with a Shimadzu UV-2401 PC spectrophotometer. The ligand concentration was in the range 10^{-5} to 1.2×10^{-5} M. The titration was continued to the point where further spectral changes were negligible, and the value of the metal cation to ligand ratio at this point was dependent on the stability of the complexes. The data thus obtained were treated with the program Specfit.[33] Statistical analysis performed by this program enabled us to determine the best model.

Microcalorimetry. Microcalorimetric titrations were performed using the 2277 thermal activity monitor microcalorimeter (Thermometric). Seventeen 15 μL portions of the metal solution were added to the cell containing 2.5 mL of 9×10^{-4} to 7×10^{-3} M solutions of ligand **1** or **2** in the appropriate solvent at 25 °C. The heat changes were measured after each addition. Chemical calibration was made by determination of the complexation enthalpy of Rb(I) with 18C6 in methanol.[34] Values of the overall stability constants (β) and of the enthalpies of complexation (ΔH) were refined simultaneously from these data using the ligand binding analysis program DIGITAM version 4.1[35] and after correction of dilution heat effects determined in separate experiments by adding the metal salt solutions to 2.5 mL of the pure solvent. The corresponding overall entropies of complexation (ΔS) were calculated from the expression $\Delta G = \Delta H - T\Delta S$, knowing that $\Delta G = -RT \ln \beta$.

Kinetic Studies. The stopped-flow technique (Applied-Photophysics, SX 18MV spectrophotometer) was used to study the rates of complexation of La(III), Eu(III), and Yb(III) with the ligand $CyMe_4$-BTPhen **2**. The absorbance versus time was followed at a suitable wavelength, which was selected on the basis of spectral changes observed in the equilibrium studies. Ligand and Ln(III) solutions prepared in methanol in the presence of Et_4NNO_3 ($I = 10^{-2}$ M) were mixed at 25.0 ± 0.2 °C in a 1 cm optical cell (mixing time = 3 ms). The ligand concentrations were around 10^{-4} M, and Ln(III) was in sufficient excess to ensure pseudo-first-order conditions ($[Ln^{3+}]_{tot}$ at least five times $[ligand]_{tot}$: 5×10^{-4} M < $[Ln^{3+}]_{tot}$ < 2.2×10^{-3} M). For each ratio, the measurement of the absorbance versus time was repeated at least five times, and the corresponding kinetic traces were treated with the program Specfit in order to obtain the value of the observed pseudo-first-order rate constants k_{obs}.[33] Variations of k_{obs} with the concentration of Ln^{3+} were fitted to a linear regression. Fisher's F test was used to check the linearity of these curves. The value of the intercept was compared to zero by a Student's t test at the 95% confidence level. The confidence intervals given in Table 2 correspond to the standard deviations obtained from independent determinations.

NMR Titrations and Stability Constant Determination. Stock solutions (0.01 M) of the ligands **1** and **2**, and of the metal nitrate salts $La(NO_3)_3 \cdot 6H_2O$, $Lu(NO_3)_3 \cdot 6H_2O$, $Eu(NO_3)_3 \cdot 5H_2O$, $Ce(NO_3)_3 \cdot 6H_2O$, and $Y(NO_3)_3 \cdot 6H_2O$ (Aldrich), were prepared in CD_3CN (Aldrich). A 0.5 mL aliquot of the appropriate ligand solution was placed in an NMR tube, and the ^1H NMR spectrum was recorded at 400.1 MHz on a Bruker AMX400 instrument. The appropriate lanthanide salt solution was added to the NMR tube in 50 μL aliquots (i.e., 0.1 equiv each time) using a calibrated Eppendorf 100 μL micropipette. The tube was inverted several times to ensure full mixing, and the ^1H NMR spectrum was recorded after each successive addition until the resonances of the free ligand had completely disappeared and/or until no further spectral changes were observed. Homogeneous solutions were obtained after each addition. The relative ratios of the different species present were calculated from the relative integrals of a suitable one-proton resonance of the ligand **1** or **2**. These values were normalized such that, for a given one-proton resonance, the total integration for all species present equaled unity. The species distributions at different metal/ligand ratios were calculated from these normalized relative ratios. The model used for the description of a given complexation reaction consists of two balanced equations (one for ligand **1** or **2**, and the second one for the metal) and equations for one or two equilibrium constants (stability constants). The Newton–Raphson[36] multidimensional nonlinear regression procedure was used to solve this set of equations to determine the values of the stability constants. In the course of regression, the experimentally determined data were fitted (compared) with the calculated data, and finally, the so-called goodness-of-fit was evaluated by the χ^2-test. The value of χ^2 is used for calculating the WSOS/DF criterion (weighted sum of squares of deviations of the experimental values from the calculated values, divided by degrees of freedom).[37] A value of WSOS/DF ≤ 20 indicates a good agreement between the experimental and calculated data. The code used for the calculation, PMeBTBP4.fm (Code Package STAMB-2013), was constructed using the software product FAMULUS.[38] The procedure has been reported previously (see Supporting Information for details).[39]

RESULTS AND DISCUSSION

Molecular Modeling. When trying to understand the binding characteristics of N-donor extractant ligands, an important aspect is to determine the types of conformers that will dominate in solution. These conformers will influence the efficiency of the extraction process because the closer the free molecule states are to the metal–ligand complex, the easier the binding process becomes. The conformer distribution is dependent on a number of factors including the repulsive interactions between the groups in the molecules, the solvent, and the concentration.

Conformer space can be searched by calculating the energies of molecules as a function of the torsion angle with either classical or quantum approaches. If several rotatable bonds are present, there will be an interdependence of the torsion angles which must be accounted for in the search. The space can be searched either systematically by varying specific angles in sequence or through a Monte Carlo approach, which generates random structures to search the conformation space. The advantage of the former method is that it can assess the interdependence of multiple torsions in a systematic way. However, for larger, more flexible molecules the number of possible conformations can rapidly increase to unreasonable levels, and the Monte Carlo approach becomes the only solution. The results from such conformer searches can be plotted graphically to understand which conformers will dominate and the energetics for transition between them. The best examples of such calculations are the Ramachandran diagrams used in the study of proteins.[40]

In the present study we have used a systematic conformer analysis to study the energetics of possible conformations that $CyMe_4$-BTBP **1** and $CyMe_4$-BTPhen **2** may adopt. The aim is to suggest the likely conformers that may exist in solution and how these will influence the chelation properties of the molecules. We also present calculations of the geometric and electronic properties of $CyMe_4$-BTPhen **2** which has previously not been studied.

dx.doi.org/10.1021/ic3026842 | Inorg. Chem. 2013, 52, 4993–5005

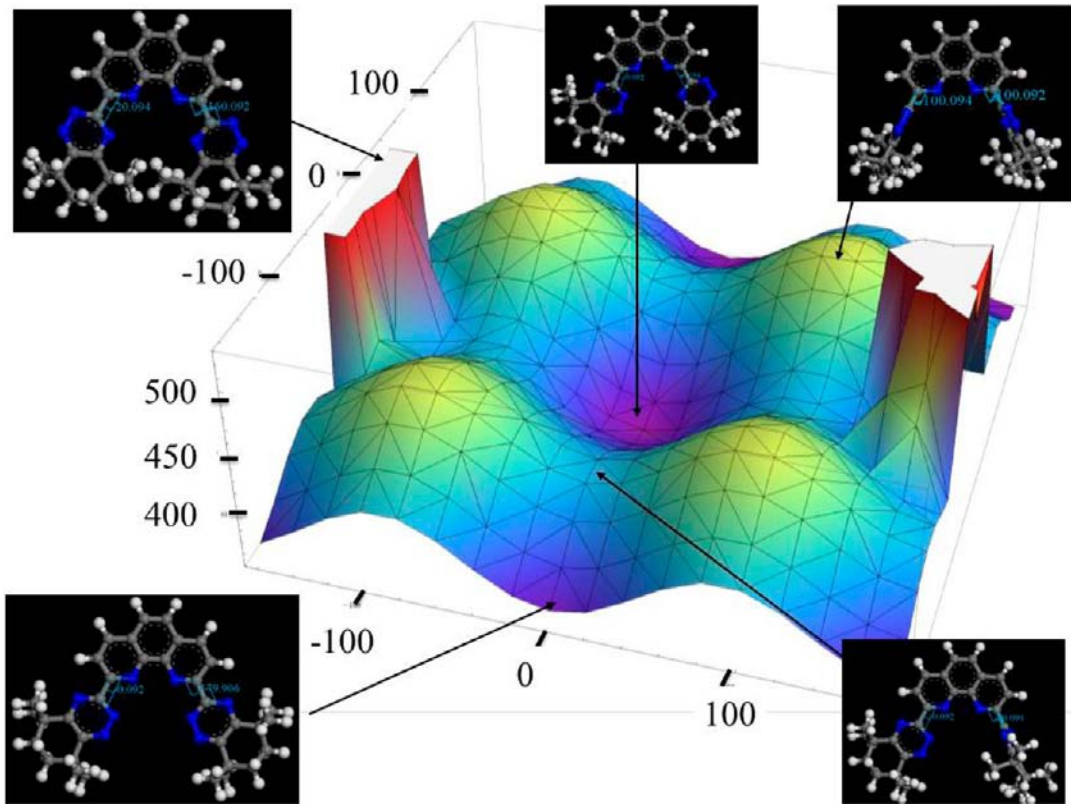

Figure 2. Energy profiles concerning the conformations of $CyMe_4$-BTPhen **2**.

The 3D structure of $CyMe_4$-BTBP **1** is shown in the Supporting Information. There are three torsion angles that control the overall structure of the molecule (these are shown on the diagram). The angles were varied systematically in steps of 30° and the energy calculated using the COMPASS forcefield,[26] with the potential cutoff set to 20 Å. A total of 1722 conformers were generated and subsequently optimized using the DMol code using the COARSE setting (which sets the tolerances for parameters such as the optimizer, number of SCF cycles, exact details are in the Supporting Information) and the BLYP functional. Using finer tolerances would risk taking some of the samples out of a metastable conformation into the global minimum which would not be desirable and significantly alter the torsion angle.

It is clear that the central torsion angle of **1** will control conformations that are relevant to binding. If this angle is close to zero, the molecule will adopt an eclipsed structure, which is seen in the crystal structures of the bound metal complexes.[7e,19,20] If this torsion angle is close to −180° or 180°, the molecule will adopt a linear conformation.

A plot of the relative energy as a function of this angle for all of the different conformers of **1** is presented in the Supporting Information. The results indicate that a large proportion of the molecules in solution will adopt linear conformations since these have the lowest energies. The linear conformations are more stable by about 12 kcal mol^{-1}. This can be seen from the line that highlights the lowest energy conformations. A linear conformation minimizes the steric repulsion between the bulky aliphatic triazine substituents. This is in broad agreement with previous work on the conformers of the BTBPs.[41] X-ray crystallographic studies reported in this paper showed that BTBP derivatives adopted linear conformations in the solid state. In addition, computational calculations in the same paper on only the BTBP core show that the all *cis*-conformation is approximately 9.5 kcal mol^{-1} higher in energy, which is similar to our calculations on the larger $CyMe_4$-BTBP ligand **1**.

The search of conformational space shows that there is a metastable conformation at about 40° which is about 8.7 kcal mol^{-1} higher in energy than the linear molecule. It could be speculated that the chelation of metal ions to $CyMe_4$-BTBP **1** involves these metastable conformations. Initially, the metal ion chelates to one side of the molecule. At this point, the energy gained by all of the nitrogen atoms coordinating to the metal ion would be larger than the steric penalty of the bulky side groups being closer together. A spreadsheet containing all of the raw data is provided as part of the Supporting Information.

The 3D structure of $CyMe_4$-BTPhen **2** is also shown in the Supporting Information. There are only two torsion angles that can significantly alter the molecular geometry; these are associated with the two C−C bonds that link the two triazine rings to the phenanthroline core. As with its BTBP equivalent **1** the torsion angles were varied in 10° steps and the energy calculated with the COMPASS forcefield.[26] In total, 324 conformers were generated. Given the relative rigidity of the molecule no further geometry optimization of these was deemed to be required and would actually be counterproductive as many of the conformers are metastable states. However, as will be discussed later, DFT was used to optimize several of the conformers to obtain better absolute energy values. Again, this was carried out with the DMol code using the BYLP functional and FINE settings for the tolerances.

The phenanthroline moiety of **2** reduces the degree of conformational variability compared to its BTBP counterpart, and only the C−C bonds that link it to the triazine groups can rotate freely. This may explain the improved kinetics of extraction of $CyMe_4$-BTPhen **2** since it is largely preorganized

dx.doi.org/10.1021/ic3026842 | *Inorg. Chem.* 2013, 52, 4993−5005

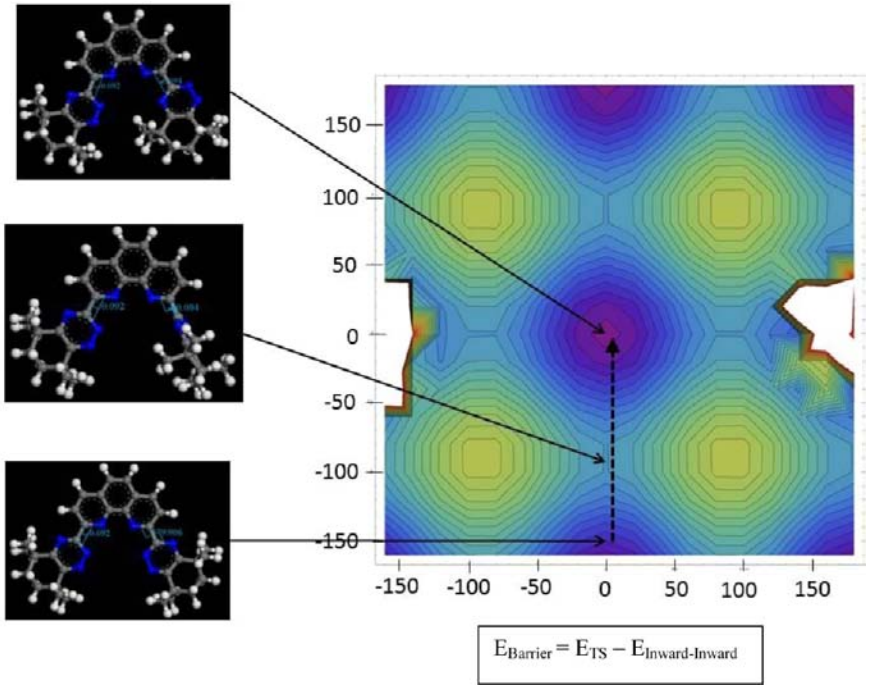

Figure 3. Transition path between rotational conformers of $CyMe_4$-BTPhen **2**.

in the ligating conformation. Figure 2 shows the result of the forcefield based conformer energy calculations and highlights the interdependence of these two torsion angles. The lowest energy configuration is that in which one of the lone pairs on nitrogen 2 of the 1,2,4-triazine ring is pointing toward the center of the molecule and the corresponding nitrogen on the second 1,2,4-triazine ring is pointing outward (termed the inward−outward configuration). The second lowest (by about 0.4 kcal mol^{-1}) is one where both of these nitrogen lone pairs are pointing in toward the center of the molecule (referred to as the inward−inward configuration). Interestingly, the conformer where both sets of adjacent nitrogens on the triazine rings are pointing outward is highly unfavorable. This is a result of the triazine ring being slightly asymmetric compared with a benzene ring, owing to the difference in length between the C−N, N−N, and C−C bonds. Thus, when the N−N bond is pointing outward, the aliphatic cyclohexenyl groups are much closer together compared to when the triazine N−N unit is pointing inward.

The difference between the two lowest energy conformations (inward−inward and inward−outward) is close enough that they are both within the accuracy limits of forcefield calculations. Thus, we optimized both of these structures using DFT to calculate more accurate energy differences which show that the inward−inward state is actually slightly more favorable (by about 4.1 kcal mol^{-1}). This is in agreement with the experimental X-ray structures of $[Eu(CyMe_4\text{-}BTPhen)_2(NO_3)]\cdot[Eu(NO_3)_5]$ and $[Eu(CyMe_4\text{-}BTPhen)_2(H_2O)](NO_3)_3\cdot 9H_2O$ which each show the $CyMe_4$-BTPhen ligand **2** in the inward−inward configuration.[12,19] As the relative stability of the inward−inward and inward−outward conformers is largely determined by steric factors, it would appear that there is a trade-off between hindrance resulting from proximity of the two $CyMe_4$-moieties in the inward−inward conformer and that resulting from one $CyMe_4$-moiety interacting with the phenanthroline proton *ortho* to the triazine ring in the inward−outward conformer.

Even with DFT based calculations the energy difference between these states is very close, and it would be feasible that both states could exist in solution depending on the temperature. Hence, it would be useful to understand the mechanism and energetics of the conversion between the two states. Using the data in Figure 2 we can determine the path of the rotation as being a direct transition with only one of the triazine rings rotating. Therefore, the rotational energy barrier can be calculated by determining the energy of the highest point on this path (the transition state E_{TS}) and subtracting the lowest energy state ($E_{Inward-Inward}$). The results are shown graphically (along with the mechanism) in Figure 3. Using the same DFT settings as those for the inward−inward and inward−outward state, we calculate the rotational barrier as being approximately 25.28 kcal/mol. This value is relatively high, but it should be borne in mind that the calculations are done in vacuum at absolute zero. This barrier will no doubt decrease in the presence of a solvent and at room temperature, and so should be regarded as an upper limit to the rotation barrier.

Geometric and Electronic Properties of $CyMe_4$-BTPhen 2. Computational chemistry enables the analysis of the geometric and electronic features of molecules. Here we present some of the calculated geometric and electronic properties of $CyMe_4$-BTPhen **2**. The solvent accessible surface and the N−N distances within the molecular cavity for both of the conformers of **2** are shown in the Supporting Information. The solvent accessible surface is the surface area of a molecule that is accessible to an external solvent molecule; it takes into account the van der Waals radius of both the ligand and solvent atoms. The method was originally developed to look at the characteristics of pockets within biomolecules.[42] It is clear from the surface that the coordination cavity of the inward−inward conformer is larger and the mouth less sterically hindered when compared with the inward−outward conformer. A more quantitative analysis of N−N distance in both the conformers shows this in more detail. As discussed earlier, the asymmetry

dx.doi.org/10.1021/ic3026842 | *Inorg. Chem.* 2013, 52, 4993−5005

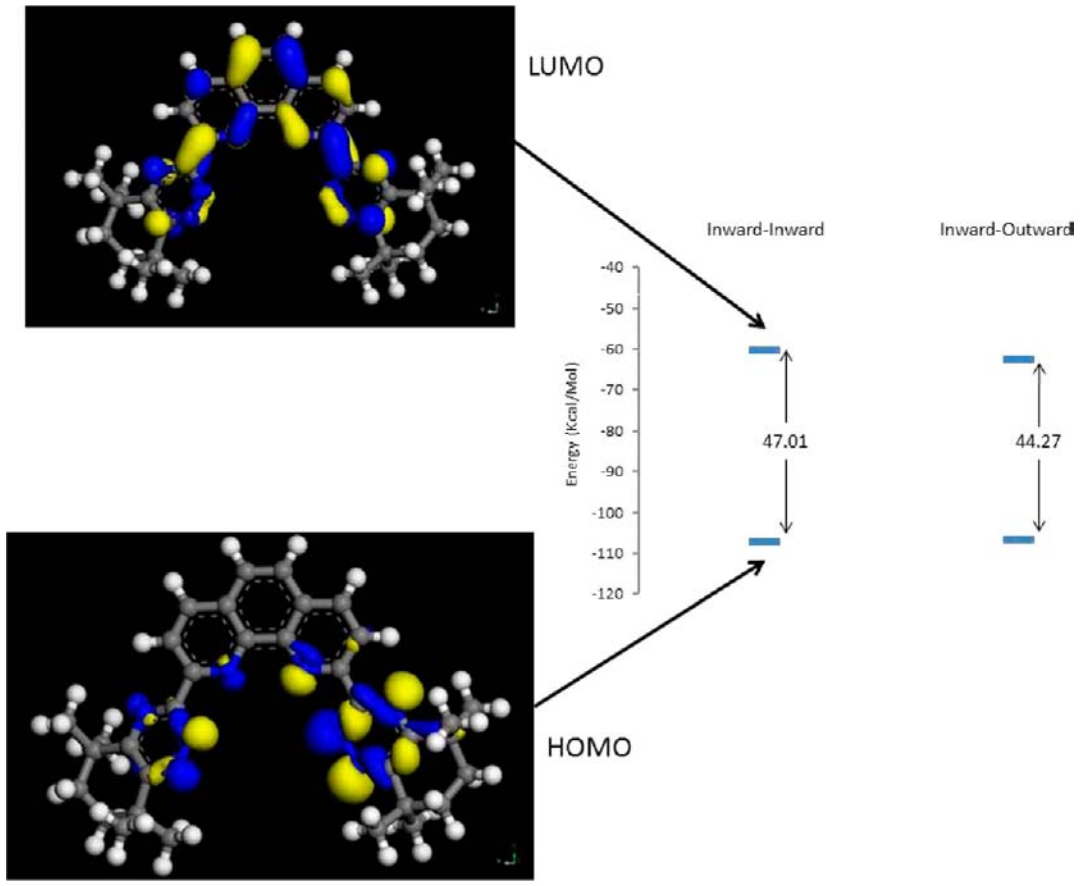

Figure 4. Molecular orbital energy level diagram for $CyMe_4$-BTPhen **2**.

within the triazine rings results in N−N distances in the inward−outward conformer being smaller, and hence a smaller volume when compared with the inward−inward conformer which has larger N−N distances. The biggest difference is at the mouth of the cavity which is approximately 0.7 Å larger in the inward−inward configuration. Thus, it would be very difficult for the metal ion to bind to the inward−outward conformer as the cavity is inaccessible from the exterior of the molecule.

The shape and energies of the frontier orbitals (the HOMO and LUMO) for the inward−inward conformer of **2** (the conformation adopted when binding to An(III) and Ln(III)) are shown in a molecular orbital diagram (Figure 4). The HOMO−LUMO gap for the inward−inward conformation is calculated to be approximately 47 kcal mol^{-1} (about 2.04 eV), and the gap is slightly less for the outward−inward conformation at about 44 kcal mol^{-1} (1.92 eV). This difference may be attributable to small changes in the electron density between the conformers. However, further studies would be required. The values for the HOMO−LUMO gap of **2** are comparable with those of $CyMe_4$-BTBP **1** for which the HOMO−LUMO gap is calculated to be 2.13 eV.[41] The calculations by Foreman et al. were carried out using the ADF code and TZP basis set on several BTBP derivatives.[41] The HOMO−LUMO gaps for these molecules ranged from 2.28 to 2.13 eV. Given the differences in their calculation methods and the structural similarities between molecules **1** and **2**, one could speculate that the HOMO−LUMO gaps of the BTPhen class of molecules could be very close to their BTBP equivalents.

The HOMO orbitals of **2** mainly reside on the triazine rings with small amounts on the nitrogen atoms in the phenanthroline ring. The LUMO also shows some probability on the triazine, but also includes a significant proportion on the carbon atoms in the phenanthroline ring. These shapes are in broad agreement with the DFT work of Bhattacharyya on the related ligand 2-(5,6-dimethyl-1,2,4-triazin-3-yl)-1,10-phenanthroline.[43] Thus, the majority of the electron donation to the metal ions is likely to occur via the 1,2,4-triazine rings. It could be speculated that, for a purely electrostatic interaction between the metal ions and the ligand, only the HOMO would play a role. However, the LUMO would also play a role in the π-backbonding interaction with the metal, which would be slightly greater for the minor actinides Am(III) and Cm(III) than the rare earths such as Eu(III).[44]

Thermodynamic Studies. The complexation of $CyMe_4$-BTPhen **2** with various lanthanide (La(III), Eu(III), and Yb(III)) nitrates and yttrium(III) nitrate was investigated in solution using UV-absorption spectrophotometry and titration microcalorimetry (ITC). The first experiments performed in methanol, a solvent in which the related BTBPs were studied previously,[21] suggested the formation of ML_2 complexes (M = metal cation, L = ligand). However, it was necessary to assume the formation of additional species to interpret satisfactorily the experimental data obtained by both techniques (see Supporting Information). Species like ML_4, M_3L_4, or even $ML_{2.5}$ complexes were found to give good fits. These results contrast with those obtained for the BTBPs, for which the experimental data unambigously agreed with the formation of both ML and ML_2 species.[21] Some ESI-mass spectra were run in methanol with some lanthanides in order to confirm or dismiss the possible formation of these species, which seems quite unlikely with a

dx.doi.org/10.1021/ic3026842 | Inorg. Chem. 2013, 52, 4993−5005

Table 1. Overall Stability Constants (log β) and Thermodynamic Parameters (in kJ mol^{-1}) for the Complexation of Some Lanthanide Cations and Y(III) with CyMe$_4$-BTPhen 2 in Acetonitrile at 25 °C

cation	complex	log β	$-\Delta G$	$-\Delta H$	$T\Delta S$
La(III)	1:2	8.5 ± 0.2	48 ± 1	85 ± 2	−37 ± 3
	1:2[a]	8.6 ± 0.2[a]	49 ± 1[a]	79 ± 3[a]	−30 ± 4[a]
Eu(III)	1:2	8.1 ± 0.1	46.2 ± 0.6	113 ± 6	−67 ± 7
Yb(III)	1:2	8.9 ± 0.1	50.7 ± 0.6	92 ± 3	−41 ± 4
Y(III)	1:2	8.5 ± 0.4	48 ± 2	87 ± 1	−39 ± 3

[a]Results for the complexation of La(III) by CyMe$_4$-BTBP **1** in acetonitrile at 25 °C.

rigid ligand such as CyMe$_4$-BTPhen **2**. The spectrum recorded for CyMe$_4$-BTPhen **2** in the presence of La(NO$_3$)$_3$ (C_{La}/C_L = 1.1) suggested only the formation of $[2L + La]^{3+}$ and $[2L + La + NO_3]^{2+}$ species. Peaks corresponding to the ligand complexed with Na(I) and Ca(II) were also visible. In the presence of Eu(NO$_3$)$_3$ (1.1 equiv), a peak corresponding to $[2L + Eu]^{3+}$ was observed. Thus, the presence of these unusual species was not indicated by ESI-mass spectrometry.

In view of the difficulties encountered in methanol, the complexation of CyMe$_4$-BTPhen **2** with the above cited metal cations was then investigated by spectrophotometry and microcalorimetry in the nonprotic solvent acetonitrile. Although the spectral changes undergone by the ligands upon addition of the various nitrates were more pronounced than in methanol (see Supporting Information), spectrophotometry proved again to be of no use for the characterization of the complexes formed in this medium.

In contrast, microcalorimetry led to interesting results. With the three lanthanides, the profiles of the thermograms were very similar, showing exothermic peaks becoming progressively more and more endothermic above a ratio C_M/C_L of ca. 0.5. The intensity of these peaks decreased to reach values corresponding to the dilution after a ratio C_M/C_L of ca. 1. The case of lanthanum is presented in the Supporting Information.

These thermograms, showing at least two phenomena, could be interpreted by the formation of ML_2 complexes. There is also evidence for the formation of a second species occurring at higher metal ion concentrations which could be an ML species, but it was not possible to derive accurately the corresponding thermodynamic parameters. In the case of yttrium, the first part of the thermogram is well fitted by considering an ML_2 complex.

The values of the stability constants (log β) and of the thermodynamic parameters ($-\Delta H$ and $T\Delta S$) are given in Table 1. The behavior of CyMe$_4$-BTPhen **2** toward the three lanthanides and yttrium is the same, i.e., the formation in all cases of 1:2 species of similar stability. No selectivity is therefore observed in the lanthanide series. A similar behavior has been observed in our previous study on lanthanide complexation by BTPs performed in methanol,[21] although in other studies a significant difference in complex stability between the Pr(III) and Eu(III) complexes of CyMe$_4$-BTPhen **2** ($\Delta\log\beta$ = 3.8 in MeOH),[19] and between the La(III) and Yb(III) complexes of the BTPs ($\Delta\log\beta$ = 4.3 in H$_2$O/MeOH)[8f] was observed. The complexation of these metal cations is characterized by strongly negative and favorable enthalpy changes ($-\Delta H > 0$) overcoming negative unfavorable entropy terms ($T\Delta S < 0$). These observations suggest strong ligand−cation interactions (in agreement with the poor solvating properties of acetonitrile), and reorganization of the ligand during complexation, respectively. The 1:2 complexes of La(III) with ligands **1** and **2** have almost identical stabilities, although there appears to be a greater enthalpy contribution to complex formation with **2** than with **1**. The thermodynamic parameters determined for Y(III) are very similar to those of the lanthanide complexes.

Kinetic Studies. The kinetics of the complexation of Ln(III) cations with CyMe$_4$-BTPhen **2** was then studied under experimental conditions identical to those used earlier on CyMe$_4$-BTBP **1**, C5-BTBP **3**, and *n*-Pr-BTP **4** (Figure 5).[21] A comparison was also made with the pentadentate ligand CyMe$_4$-BTTP **5** (Figure 5).[45] The kinetics of complexation of La(III), Eu(III), and Yb(III) with CyMe$_4$-BTPhen **2** was followed by UV spectrophotometry using the stop-flow technique under pseudo-first-order conditions. The absorbance at a wavelength corresponding to the maximum overall change was monitored versus time for different metal concentrations (5−22 times the concentration of the ligand).

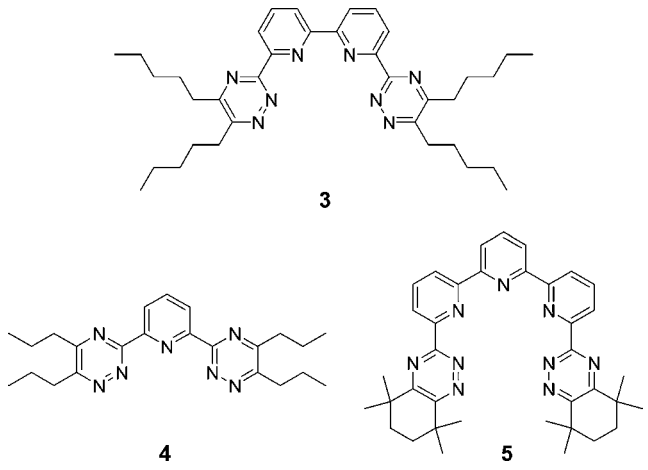

Figure 5. Structures of the ligands C5-BTBP **3**, *n*-Pr-BTP **4**, and CyMe$_4$-BTTP **5**.

The experimental kinetic trace recorded for the complexation of Eu(III) with CyMe$_4$-BTPhen **2** is shown in Figure 6. For Eu(III) and Yb(III) the time dependence of the absorbance at 365 nm was well fitted by a single exponential function. The observed pseudo-first-order rate constants (k_{obs}'s) vary linearly with $[Ln]_{tot}$ with a non-significant intercept (Figure 7). In these cases only the values of the formation rate constants (k_f's) could be determined (Table 2).

In the case of La(III), the absorbance at t = 0 s increased with the excess of metal. This behavior is typical of a very fast reaction, resulting in a loss of information at the early stages and preventing any interpretation of the kinetic traces. However, it could be assumed that for La(III) the complexation kinetics with **2** are more rapid than those of Eu(III) and Yb(III).

dx.doi.org/10.1021/ic3026842 | Inorg. Chem. 2013, 52, 4993−5005

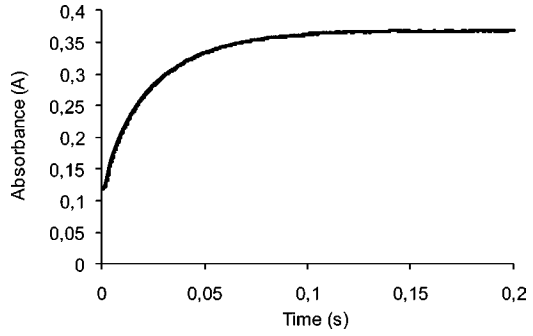

Figure 6. Experimental kinetic trace for the complexation of $Eu(NO_3)_3$ (C_M = 5.51 × 10^{-4} M) with $CyMe_4$-BTPhen **2** (C_L = 1.09 × 10^{-4} M) in methanol (λ = 365 nm, T = 25 °C, I = 10^{-2} M Et_4NNO_3).

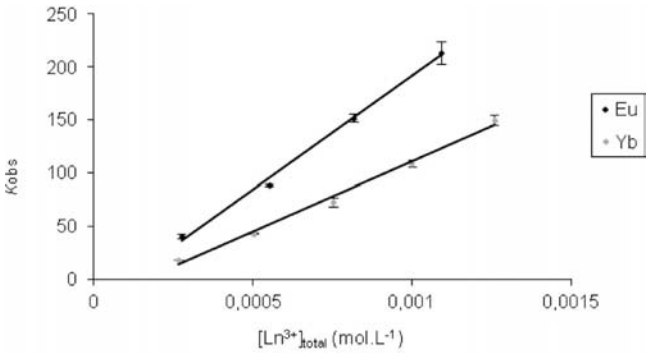

Figure 7. Observed pseudo-first-order rate constants (k_{obs}'s) as a function of the total metal ion concentration for the complexation of $CyMe_4$-BTPhen **2** with Eu(III) and Yb(III) in methanol at 25 °C.

Table 2. Formation Rate Constants (10^3 L mol^{-1} s^{-1}) for the Complexation of Lanthanides with Aromatic Nitrogen Donor Ligands in Methanol at 25 °C

ligand	La(III)	Eu(III)	Yb(III)
$CyMe_4$-BTPhen **2**	*a*	215 ± 10	129 ± 3
$CyMe_4$-BTTP **5**	14.7 ± 0.3	2.0 ± 0.2	0.29 ± 0.02
C5-BTBP **3**	223 ± 1	27.0 ± 0.3	4.07 ± 0.07
$CyMe_4$-BTBP **1**	70.5 ± 0.8	11.5 ± 0.8	1.4 ± 0.1
n-Pr-BTP **4**	182 ± 5	*a*	118.7 ± 0.9

[a]Kinetic traces not interpretable.

For the complexation of the same lanthanide cations by $CyMe_4$-BTTP **5**, the time dependence of the absorbance at 350 nm was also well fitted by a single exponential function (see Supporting Information for the case of lanthanum). Linear regression of the variations of k_{obs} with $[Ln]_{tot}$ led to the values of k_f (Table 2).

For all systems studied including *n*-Pr-BTP **4** and BTBPs **1** and **3**, the trend observed is a decrease of the k_f values across the lanthanide series (e.g., in the case of $CyMe_4$-BTPhen **2**: k_f[Eu(III)] = 1.7 k_f[Yb(III)]), in line with the lanthanide contraction. The stronger solvation of the cations at the end of the series could explain this decrease. For a given cation, the rate constants decrease in the following sequence:

$CyMe_4$-BTPhen **2** > *n*-Pr-BTP **4** > C5-BTBP **3** > $CyMe_4$-BTBP **1** > $CyMe_4$-BTTP **5**

In other words, the complexation reaction is much faster with the more rigid preorganized ligand $CyMe_4$-BTPhen **2** than with $CyMe_4$-BTBP **1** and especially $CyMe_4$-BTTP **5** (ca. 92 times and 444 times faster, respectively, with Yb(III)), which exhibits the slowest complexation kinetics among the five ligands studied. This observation is fully in agreement with the extraction kinetics results for ligands **1** and **2**.[12] One of the principal criticisms of $CyMe_4$-BTBP **1** as a ligand for the SANEX process has been that the rates of extraction are too slow for use in an industrial process. Clearly, the $CyMe_4$-BTPhen molecule **2** exhibits much improved rates of extraction. These differences in rates of complexation can be understood in terms of the number of biaryl dihedral angles that each ligand needs to adjust in order to achieve the correct conformation for complex formation. Thus, $CyMe_4$-BTPhen **2** (and *n*-Pr-BTP **4**), which has only two dihedral angles to adjust (i.e., those between the pyridine or phenanthroline moieties and the outer 1,2,4-triazine rings), complexes the metal ions more rapidly than BTBPs **1** and **3** (which each have three dihedral angles to adjust) or $CyMe_4$-BTTP **5** (which has four dihedral angles to adjust).

NMR Titrations and Stability Constant Determination. In order to clarify the results observed above for the complexation of $CyMe_4$-BTBP **1** and $CyMe_4$-BTPhen **2** with the lanthanides by titration microcalorimetry and gain further insight into the solution speciation of these ligands, we carried out some NMR titrations of both ligands with Y(III) and the diamagnetic lanthanides La(III) and Lu(III).[46] We have previously employed this method to investigate the solution speciation of a related quadridentate ligand with the lanthanides.[47] During the ^{1}H NMR titration of $CyMe_4$-BTPhen **2** with $La(NO_3)_3$ in deuterated acetonitrile, both 1:1 and 1:2 M:L species were observed during the course of the titration. Initially, a single species was observed at the beginning of the titration, and the disappearance of the free ligand resonances after 0.6 equiv of La(III) had been added indicates this was a 1:2 species. The 1:2 species was the dominant species observed throughout the titration, but small amounts of the 1:1 species (formed by dissociation of the 1:2 complexes) were observed at higher metal/ligand ratios. The species distribution curve for the titration of **2** with $La(NO_3)_3$ is presented in Figure 8. The NMR stack plots are shown in the Supporting Information.

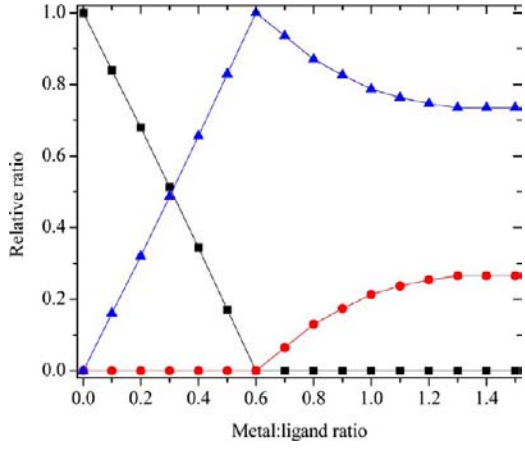

Figure 8. ^{1}H NMR titration of $CyMe_4$-BTPhen **2** with $La(NO_3)_3$ in CD_3CN (key: black ■ = free ligand **2**, red ● = 1:1 complex, blue ▲ = 1:2 complex).

dx.doi.org/10.1021/ic3026842 | Inorg. Chem. 2013, 52, 4993−5005

Similar results were obtained for the titrations of $CyMe_4$-BTPhen **2** with $Lu(NO_3)_3$ and $Y(NO_3)_3$ (see Supporting Information), although in the case of $Y(NO_3)_3$, very minor amounts of the 1:1 complex were observed at high metal/ligand ratios, suggesting that the 1:2 complex of **2** with Y(III) is more stable and dissociates less readily than those of La(III) and Lu(III). These results are in contrast to those previously obtained for a related quadridentate ligand which did not extract Am(III) or Eu(III) from nitric acid solutions (in contrast to **1** and **2**), and for which 1:1 species were the major solution species observed by NMR titrations with lanthanide nitrates.[47] The ^{1}H NMR titrations of **2** with the paramagnetic lanthanides Eu(III) and Ce(III) led only to the formation of 1:2 complexes in each case, and the very low intensities of the resonances for these complexes did not allow us to calculate the species distribution curves. The 1:2 stoichiometry observed by NMR for the complexation of lanthanides and yttrium by **2** is in agreement with that determined by microcalorimetry.

Slow evaporation of the CD_3CN solution used for the NMR titration of **2** with $Y(NO_3)_3$ led to the formation of crystals suitable for X-ray crystallographic analysis. Surprisingly, the charge neutral 1:1 complex $[Y(\mathbf{2})(NO_3)_3]$.MeCN was isolated and structurally characterized (Figure 9) rather than the

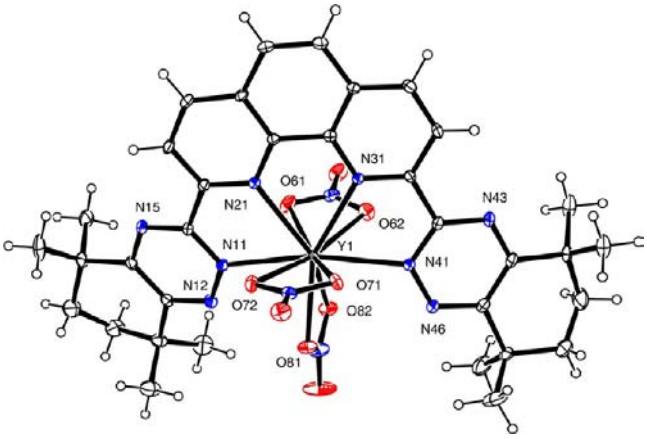

Figure 9. X-ray crystal structure of $[Y(\mathbf{2})(NO_3)_3]$·MeCN with ellipsoids at 30% probability. The solvent molecule has been omitted for clarity.

expected 1:2 complex. This is unusual as only solid state structures of 1:2 complexes of BTPhens with the lanthanides have been reported to date.[12,19] The metal ion is 10-coordinate being bonded to the tetradentate ligand **2** and to three bidentate nitrate ions. The tetradentate ligand is approximately planar with angles between consecutive rings of 16.4(2)°, 6.4(2)°, 9.7(2)°, respectively. The Y−N distances are similar in the range 2.497(3)−2.526(3)Å. The structure has approximate mirror symmetry. Thus, the plane of the metal and the three nitrate nitrogen atoms is approximately perpendicular at an angle of 88.8(1)° to the equatorial plane of the metal and the four ligand donor nitrogen atoms. The Y−O distances are Y(1)−O(82) 2.378(2), Y(1)−O(81) 2.381(2), Y(1)−O(71) 2.431(2), Y(1)−O(72) 2.530(2), Y(1)−O(61) 2.535(3), Y(1)−O(62) 2.535(3) Å. The structure is very similar to that of the 1:1 complex of $CyMe_4$-BTBP **1** with $Eu(NO_3)_3$,[19,20] and with those of other BTBPs with Ln(III) reported previously.[41]

The ^{1}H NMR titrations of $CyMe_4$-BTBP **1** with La(III), Lu(III), and Y(III) gave very similar results to those of $CyMe_4$-BTPhen **2**. The 1:2 bis-complexes were again the major solution species observed, especially at low metal/ligand ratios. At higher metal/ligand ratios, the bis-complexes begin to dissociate leading to the formation of 1:1 complexes. The species distribution curve for the titration of **1** with $Y(NO_3)_3$ is shown in Figure 10 as an example (see the Supporting

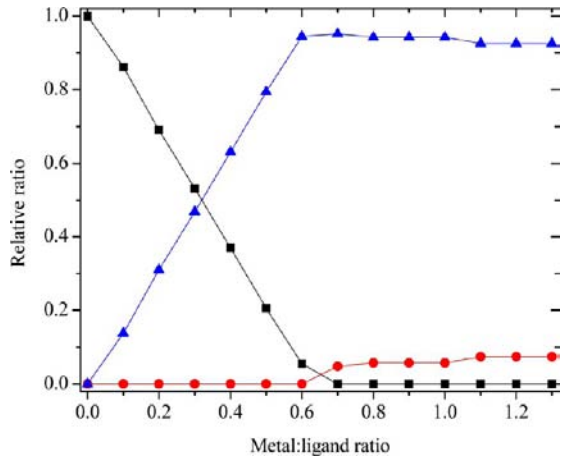

Figure 10. ^{1}H NMR titration of $CyMe_4$-BTBP **1** with $Y(NO_3)_3$ in CD_3CN (key: ■ = free ligand **1**, red ● = 1:1 complex, blue ▲ = 1:2 complex).

Information for NMR stack plots for the titrations of **1** with La(III), Lu(III), and Y(III)). Interestingly, in the titration of **1** with $Lu(NO_3)_3$, greater amounts of the 1:1 complex were observed earlier on in the titration than was the case in the other titrations (at a metal:ligand ratio of 0.2). The similar solution speciation of **1** and **2** with the lanthanides observed by NMR suggests that the differences in extraction capability between the two ligands (about 2 orders of magnitude higher distribution ratios for **2**) are not related to differences in the stoichiometries of their extracted metal complexes. Recent lanthanide speciation studies with ligands **1** and **2** in solution and in the solid state further support this view.[19] However, it remains to be seen if the similar speciation of ligands **1** and **2** with the actinides parallels that of the lanthanides.

Using a procedure reported previously,[39] the data obtained from the NMR titrations was used to calculate the stability constants for the complexation of $CyMe_4$-BTBP **1** and $CyMe_4$-BTPhen **2** with La(III), Lu(III), and Y(III).[48] In the case of $La(NO_3)_3$, "reverse" NMR titrations (i.e., addition of **1** or **2** to a solution of La(III)) were carried out to aid in the determination of the stability constants (see Supporting Information). The stability constants are presented in the Supporting Information. In the case of ligand **1**, there is a reasonably good agreement between the value for the stability constant of the 1:2 complex of La(III) with **1**, and the corresponding value obtained by microcalorimetry (Table 1). The stability constant for the 1:2 complex of **2** with Y(III) determined by NMR also agrees reasonably well with that determined by microcalorimetric titration.

We then carried out a series of lanthanide NMR competition experiments with the aim of determining whether $CyMe_4$-BTPhen **2** formed thermodynamically more stable complexes than those of $CyMe_4$-BTBP **1**. The ^{1}H NMR spectrum of a 1:1:1 mixture of $CyMe_4$-BTBP **1**, $CyMe_4$-BTPhen **2**, and $La(NO_3)_3$ in deuterated acetonitrile displayed resonances for the 1:2 bis-BTBP complex, the 1:2 bis-BTPhen complex, and

dx.doi.org/10.1021/ic3026842 | Inorg. Chem. 2013, 52, 4993−5005

an additional set of resonances (four methyl peaks in the aliphatic region, one triplet, two double doublets, one singlet, and one large singlet in the aromatic region) that were assigned to the heteroleptic 1:2 bis-complex (a bis-complex containing one $CyMe_4$-BTBP and one $CyMe_4$-BTPhen ligand). These resonances were not previously observed in the titrations of either **1** or **2** with $La(NO_3)_3$, and thus did not correspond to the 1:1 complexes observed as minor components in some cases. The approximate ratio of bis-BTBP/bis-BTPhen/heteroleptic bis-complex was 1:1:2 (the expected ratio based on statistics). A statistical mixture of three bis-complexes was thus obtained (see Supporting Information).

We then assessed the ability of each of the ligands **1** or **2** to displace the other from its lanthanide 1:2 bis-complexes. The addition of a solution of $CyMe_4$-BTPhen **2** (1 equiv) to a solution of the 1:2 bis-complex of $CyMe_4$-BTBP **1** with $La(NO_3)_3$ (formed by the addition of 1 equiv of $CyMe_4$-BTBP **1** to 0.5 equiv of $La(NO_3)_3$) gave rise to a solution containing a mixture of 1:2 bis-BTPhen and heteroleptic 1:2 bis-complexes, as well as free uncomplexed BTBP **1** (see Supporting Information). Only trace amounts of the 1:2 bis-BTBP complex were observed. The major species present was the 1:2 bis-BTPhen complex. No peaks due to free uncomplexed $CyMe_4$-BTPhen **2** were observed. Thus, $CyMe_4$-BTPhen **2** is able to displace $CyMe_4$-BTBP **1** from its 1:2 bis-complex with La(III).

A solution almost identical in composition to that above was obtained when a solution of $CyMe_4$-BTBP **1** (1 equiv) was added to a solution of the 1:2 bis-BTPhen complex with $La(NO_3)_3$. The 1:2 bis-BTPhen complex was again the major solution species present, and minor amounts of the heteroleptic 1:2 bis-complex were also observed. Thus, the addition of $CyMe_4$-BTBP **1** to a solution of the La(III) bis-complex of **2** has little or no effect. At best, **1** is able to displace one $CyMe_4$-BTPhen ligand **2** from its bis-complexes but never two. This is evidence that $CyMe_4$-BTPhen **2** must be forming the thermodynamically more stable bis-complex with La(III) than $CyMe_4$-BTBP **1**. This is, to the best of our knowledge, the only direct evidence so far of differences in the thermodynamic stabilities between the 1:2 complexes of BTBPs and BTPhens. Whether this higher complex stability is enthalpic or entropic (or both) remains unclear.

We then carried out a ^{1}H NMR titration of a 50:50 mixture of both ligands **1** and **2** with $La(NO_3)_3$ in deuterated acetonitrile. Initially, we observed the formation of the 1:2 bis-BTPhen complex and minor traces of the heteroleptic 1:2 bis-complex as the metal was added but not the 1:2 bis-BTBP complex. After 0.4 equiv of metal had been added, the free ligand $CyMe_4$-BTPhen **2** had been completely consumed. Further addition of La(III) led to the formation of the heteroleptic 1:2 bis-complex and the 1:2 bis-BTBP complex, with the heteroleptic 1:2 bis-complex being the major species. Once 0.7 equiv of metal had been added, both ligands had been completely consumed. At this stage, an equilibrium mixture of 1:2 bis-BTPhen, 1:2 bis-BTBP, and heterolepic 1:2 bis-complexes was observed, with no single species dominating (see Supporting Information). After this point, 1:1 complexes began to form. Further addition of La(III) now led to the formation of both 1:1 BTBP and 1:1 BTPhen complexes, in approximately equal amounts. After 1.5 equiv of metal had been added, a complex equilibrium mixture of 1:2 bis-BTBP, 1:2 bis-BTPhen, heteroleptic 1:2 bis-complex, 1:1 BTBP, and 1:1 BTPhen complexes was obtained (Figure 11). The relative ratio of the three bis-complexes was approximately the same as that

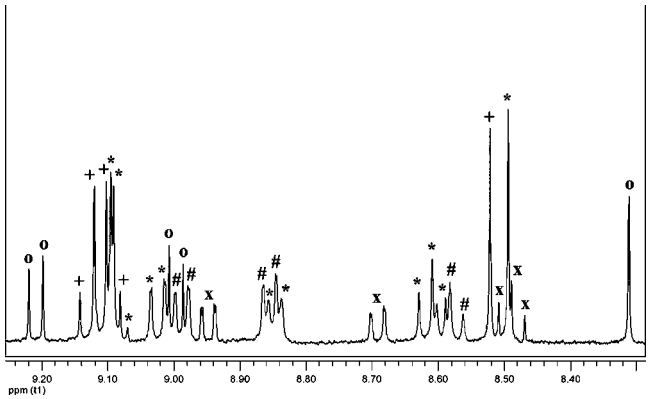

Figure 11. Enlargement of the aromatic region of the ^{1}H NMR spectrum of a 50:50 mixture of $CyMe_4$-BTBP **1** and $CyMe_4$-BTPhen **2** (1 equiv) in CD_3CN after 1.5 equiv of $La(NO_3)_3$ had been added (assignments: # = 1:2 bis-BTBP complex, + = 1:2 bis-BTPhen complex, * = heteroleptic 1:2 bis-complex, **x** = 1:1 BTBP complex, **o** = 1:1 BTPhen complex).

after 0.7 equiv of La(III) had been added, indicating that all three bis-complexes dissociated to form the 1:1 complexes. The order of appearance of the 1:2 bis-complexes early in the titration suggests that the order of stability of the 1:2 bis-complexes is

1:2 bis-BTPhen complex

> heteroleptic BTBP/BTPhen 1:2 bis-complex

> 1:2 bis-BTBP complex

Similar results were obtained in the NMR competition experiments of **1** and **2** with $Lu(NO_3)_3$. A 1:1:1 mixture of $CyMe_4$-BTBP **1**, $CyMe_4$-BTPhen **2**, and $Lu(NO_3)_3$ in deuterated acetonitrile gave rise to a statistical mixture of 1:2 bis-BTBP, 1:2 bis-BTPhen, and heteroleptic 1:2 bis-complexes in an approximate ratio of 1:1:2 (see Supporting Information). However, in contrast to La(III), no ligand displacement reaction occurred when a solution of either ligand **1** or **2** was added to a solution of the 1:2 bis-complex of the other ligand with Lu(III). This indicates that, contrary to the situation with La(III), $CyMe_4$-BTPhen **2** is unable to displace $CyMe_4$-BTBP from its Lu(III) bis-complex. The thermodynamic stabilities of the two bis-complexes could be quite similar, or the kinetic barrier to displacement of ligand **1** with ligand **2** (or vice versa) could be higher with Lu(III) than is the case with La(III). During the ^{1}H NMR titration of a 50:50 mixture of **1** and **2** with $Lu(NO_3)_3$, an almost equal mixture of 1:2 bis-BTPhen and heteroleptic 1:2 bis-complexes was formed initially (only traces of the 1:2 bis-BTBP complex were observed), and **2** was completely consumed after 0.6 equiv of Lu(III) had been added. The 1:2 complexes partially dissociated to 1:1 complexes as the metal/ligand ratio was increased, and an equilibrium mixture of 1:2 bis-BTBP, 1:2 bis-BTPhen, heteroleptic 1:2 bis-complex, 1:1 BTBP, and 1:1 BTPhen complexes was obtained after 1.5 equiv of metal had been added (see Supporting Information). The order of appearance of the bis-complexes early in the titration suggests that the order of stability of the bis-complexes with Lu(III) is the same as that found with La(III), namely

dx.doi.org/10.1021/ic3026842 | Inorg. Chem. 2013, 52, 4993−5005

1:2 bis-BTPhen complex

≥ heteroleptic BTBP/BTPhen 1:2 bis-complex

> 1:2 bis-BTBP complex

CONCLUSIONS

Density functional theory calculations show that $CyMe_4$-BTBP **1** must overcome a rotational energy barrier of *ca.* 12 kcal mol^{-1} in order to achieve its metal binding conformation, while this barrier is absent in $CyMe_4$-BTPhen **2**. For both ligands, a relatively small energy barrier exists corresponding to rotation about the outer 1,2,4-triazine rings (4.1 kcal mol^{-1} for **2**). The complexation thermodynamics and kinetics of $CyMe_4$-BTPhen **2** with some lanthanide cations have been studied in both methanol and acetonitrile. In acetonitrile, only the microcalorimetric titrations clearly showed the formation of predominant ML_2 complexes with lanthanides. However, there was evidence for the formation of one or more additional species, certainly an ML species. The fast kinetics study carried on in methanol using the stopped flow technique with a spectrophotometric detection showed that the rate of complexation of trivalent lanthanides with the aromatic *N*-donor ligands was strongly dependent on the degree of preorganization of the ligands, the fastest reaction being achieved with the ligand $CyMe_4$-BTPhen **2**. Lanthanide NMR titrations showed that 1:2 species were the major solution species formed with La(III), Lu(III), and Y(III), while lanthanide binding competition experiments in deuterated acetonitrile revealed that $CyMe_4$-BTPhen **2** formed the thermodynamically more stable 1:2 bis-complex with La(III) than $CyMe_4$-BTBP **1**. The above results suggest that differences in extraction ability between the BTBPs and their preorganized BTPhen counterparts are, in the case of lanthanides at least, based only on subtle differences in the thermodynamic stabilities of the complexes formed. It remains to be seen whether the similarities in the speciation of ligands **1** and **2** with the lanthanides are also observed with the actinides. On the other hand, BTPhens exhibit faster complexation kinetics than BTBPs that are related to the higher degree of ligand preorganization in the BTPhens. This study adds more support to the notion that the BTPhen ligands appear to be the optimal choice for the separation of Am(III) from Eu(III) within partitioning processes.

ASSOCIATED CONTENT

Supporting Information

Details of molecular modeling calculations. 3D structures of ligands **1** and **2**. Spectrophotometric and microcalorimetric titrations of $CyMe_4$-BTPhen **2** with lanthanide cations. Kinetics studies of the complexation of $CyMe_4$-BTTP **5** with lanthanides. NMR stack plots, species distribution curves and calculated and experimental molar concentrations of species present for the titrations of $CyMe_4$-BTBP **1** and $CyMe_4$-BTPhen **2** with lanthanide nitrates. Mercury plot of the crystal structure of $CyMe_4$-BTPhen **2** with $Y(NO_3)_3$. This material is available free of charge via the Internet at http://pubs.acs.org.

AUTHOR INFORMATION

Corresponding Author

*E-mail: l.m.harwood@reading.ac.uk.

Present Addresses

[⊥]Department of Chemical and Forensic Sciences, Faculty of Health and Life Sciences, Northumbria University, Newcastle upon Tyne NE1 8ST, U.K.

[#]PSE, Inc., 3 Wing Drive, Suite No. 103, Cedar Knolls, NJ 07927, USA.

Notes

The authors declare no competing financial interest.

ACKNOWLEDGMENTS

We thank the Nuclear Fission Safety Program of the European Union for support under the ACSEPT (FP7-CP-2007-211 267) contract. We also thank the EPSRC and the University of Reading for funds for the X-Calibur system. We gratefully acknowledge Bruce Hanson (NNL) for the provision of funding through NNL's Spent Fuel Signature Research program. We also acknowledge Stéphanie Petiot-Bécard, Dr. Sarah Cianférani, and Dr. Alain Van Dorsselaer (LSMBO) for ESI-MS experiments. Use of the Chemical Analysis Facility at the University of Reading is also gratefully acknowledged.

REFERENCES

(1) *Fuel Cycle Stewardship in a Nuclear Renaissance*; The Royal Society Science Policy Centre Report 10/11; The Royal Society: London, 2011 (ISBN 978-0-85403-891-6).

(2) (a) Sood, D. D.; Patil, S. K. *J. Radioanal. Nucl. Chem.* **1996**, *203*, 547−573. (b) Musikas, C.; Schultz, W.; Liljenzin, J.-O. *Solvent Extraction Principles and Practice*, 2nd ed.; Rydberg, J., Cox, M., Musikas, C., Choppin, G., Eds.; Marcel Dekker, Inc.: New York, 2004; pp 507−557. (c) Nash, K. L.; Madic, C.; Mathur, J.; Lacquement, J. *The Chemistry of the Actinide and Transactinide Elements*; Katz, J. J., Morss, L. R., Edelstein, N. M., Fuger, J., Eds.; Springer: Dordrecht, 2006; Vol. *1*, pp 2622−2798.

(3) (a) *Actinide and Fission Product Partitioning and Transmutation Status and Assessment Report*; OECD/NEA: Paris, 1999. (b) Magill, J.; Berthou, V.; Haas, D.; Galy, J.; Schenkel, R.; Wiese, H.-W.; Heusener, G.; Tommasi, J.; Youinou, G. *Nucl. Energy* **2003**, *42*, 263−277. (c) Salvatores, M. *Nucl. Eng. Des.* **2005**, *235*, 805−816. (d) Salvatores, M.; Palmiotti, G. *Prog. Part. Nucl. Phys.* **2011**, *66*, 144−166.

(4) (a) Madic, C.; Hudson, M. J.; Liljenzin, J.-O.; Glatz, J.-P.; Nannicini, R.; Facchini, A.; Kolarik, Z.; Odoj, R. *Prog. Nucl. Energy* **2002**, *40*, 523−526. (b) Madic, C.; Boullis, B.; Baron, P.; Testard, F.; Hudson, M. J.; Liljenzin, J.-O.; Christiansen, B.; Ferrando, M.; Facchini, A.; Geist, A.; Modolo, G.; Espartero, A. G.; De Mendoza, J. *J. Alloys Compd.* **2007**, *444*−*445*, 23−27.

(5) For reviews on the partitioning of minor actinides, see: (a) Nash, K. L. *Solvent Extr. Ion Exch.* **1993**, *11*, 729−768. (b) Mathur, J. N.; Murali, M. S.; Nash, K. L. *Solvent Extr. Ion Exch.* **2001**, *19*, 357−390. (c) Lumetta, G. J.; Gelis, A. V.; Vandegrift, G. F. *Solvent Extr. Ion Exch.* **2010**, *28*, 287−312. (d) Hill, C. *Ion Exchange and Solvent Extraction: A Series of Advances*; Moyer, B. A., Ed.; CRC Press: Boca Raton, FL, 2010; Vol. *19*, pp 119−193. (e) Modolo, G.; Wilden, A.; Geist, A.; Magnusson, D.; Malmbeck, R. *Radiochim. Acta* **2012**, *100*, 715−725.

(6) (a) Cotton, S. *Comprehensive Coordination Chemistry II*; McCleverty, J. A., Meyer, T. J., Eds.; Elsevier: Oxford, 2004; Vol. *3*, pp 93−188. (b) Burns, C. J.; Neu, M. P.; Boukhalfa, H.; Gutowski, K. E.; Bridges, N. J.; Rogers, R. D. *Comprehensive Coordination Chemistry II*; McCleverty, J. A., Meyer, T. J., Eds.; Elsevier: Oxford, 2004; Vol. 3, pp 189−332. (c) Katz, J. J.; Morss, L. R.; Edelstein, N. M.; Fuger, J. *The Chemistry of the Actinide and Transactinide Elements*, Vol. *1*; Katz, J. J., Morss, L. R., Edelstein, N. M., Fuger, J., Eds.; Springer: Dordrecht, 2006; pp 1−17.

(7) (a) Ekberg, C.; Fermvik, A.; Retegan, T.; Skarnemark, G.; Foreman, M. R. S.; Hudson, M. J.; Englund, S.; Nilsson, M. *Radiochim. Acta* **2008**, *96*, 225−233. (b) Kolarik, Z. *Chem. Rev.* **2008**, *108*, 4208−4252. (c) Mincher, B. J.; Modolo, G.; Mezyk, S. P. *Solvent Extr. Ion*

Exch. **2010**, *28*, 415−436. (d) Lewis, F. W.; Hudson, M. J.; Harwood, L. M. *Synlett* **2011**, 2609−2632. (e) Hudson, M. J.; Harwood, L. M.; Laventine, D. M.; Lewis, F. W. *Inorg. Chem.* **2013**, *52*, 3414−3428. (f) Panak, P. J.; Geist, A. *Chem. Rev.* **2013**, *113*, 1199−1236.

(8) See for example: (a) Drew, M. G. B.; Guillaneux, D.; Hudson, M. J.; Iveson, P. B.; Russell, M. L.; Madic, C. *Inorg. Chem. Commun.* **2001**, *4*, 12−15. (b) Iveson, P. B.; Riviére, C.; Guillaneux, D.; Nierlich, M.; Thuéry, P.; Ephritikhine, M.; Madic, C. *Chem. Commun.* **2001**, 1512−1513. (c) Boucher, C.; Drew, M. G. B.; Giddings, P.; Harwood, L. M.; Hudson, M. J.; Iveson, P. B.; Madic, C. *Inorg. Chem. Commun.* **2002**, *5*, 596−599. (d) Berthet, J.-C.; Miquel, Y.; Iveson, P. B.; Nierlich, M.; Thuéry, P.; Madic, C.; Ephritikhine, M. *J. Chem. Soc., Dalton Trans.* **2002**, 3265−3272. (e) Colette, S.; Amekraz, B.; Madic, C.; Berthon, L.; Cote, G.; Moulin, C. *Inorg. Chem.* **2002**, *41*, 7031−7041. (f) Colette, S.; Amekraz, B.; Madic, C.; Berthon, L.; Cote, G.; Moulin, C. *Inorg. Chem.* **2003**, *42*, 2215−2226. (g) Colette, S.; Amekraz, B.; Madic, C.; Berthon, L.; Cote, G.; Moulin, C. *Inorg. Chem.* **2004**, *43*, 6745−6751. (h) Drew, M. G. B.; Foreman, M. R. St. J.; Geist, A.; Hudson, M. J.; Marken, F.; Norman, V.; Weigl, M. *Polyhedron* **2006**, *25*, 888−900. (i) Hudson, M. J.; Boucher, C. E.; Braekers, D.; Desreux, J. F.; Drew, M. G. B.; Foreman, M. R. St. J.; Harwood, L. M.; Hill, C.; Madic, C.; Marken, F.; Youngs, T. G. A. *New J. Chem.* **2006**, *30*, 1171−1183. (j) Steppert, M.; Walther, C.; Geist, A.; Fanghänel, T. *New J. Chem.* **2009**, *33*, 2437−2442. (k) Benay, G.; Schurhammer, R.; Wipff, G. *Phys. Chem. Chem. Phys.* **2010**, *12*, 11089−11102. (l) Benay, G.; Schurhammer, R.; Desaphy, J.; Wipff, G. *New J. Chem.* **2011**, *35*, 184−189.

(9) See for example: (a) Drew, M. G. B.; Foreman, M. R. S. J.; Hill, C.; Hudson, M. J.; Madic, C. *Inorg. Chem. Commun.* **2005**, *8*, 239−241. (b) Nilsson, M.; Ekberg, C.; Foreman, M.; Hudson, M.; Liljenzin, J.-O.; Modolo, G.; Skarnemark, G. *Solvent Extr. Ion Exch.* **2006**, *24*, 823−843. (c) Ekberg, C.; Aneheim, E.; Fermvik, A.; Foreman, M.; Löfström-Engdahl, E.; Retegan, T.; Spendlikova, I. *J. Chem. Eng. Data* **2010**, *55*, 5133−5137. (d) Berthet, J.-C.; Maynadié, J.; Thuéry, P.; Ephritikhine, M. *Dalton Trans.* **2010**, *39*, 6801−6807. (e) Harwood, L. M.; Lewis, F. W.; Hudson, M. J.; John, J.; Distler, P. *Solvent Extr. Ion Exch.* **2011**, *29*, 551−576. (f) Distler, P.; Spendlikova, I.; John, J.; Harwood, L. M.; Hudson, M. J.; Lewis, F. W. *Radiochim. Acta* **2012**, *100*, 747−751. (g) Aneheim, E.; Grüner, B.; Ekberg, C.; Foreman, M. R.; St, J.; Hájková, Z.; Löfström-Engdahl, E.; Drew, M. G. B.; Hudson, M. J. *Polyhedron* **2013**, *50*, 154−163.

(10) Magnusson, D.; Christiansen, B.; Foreman, M. R. S.; Geist, A.; Glatz, J.-P.; Malmbeck, R.; Modolo, G.; Serrano-Purroy, D.; Sorel, C. *Solvent Extr. Ion Exch.* **2009**, *27*, 97−106.

(11) (a) Aneheim, E.; Ekberg, C.; Fermvik, A.; Foreman, M. R. St. J.; Retegan, T.; Skarnemark, G. *Solvent Extr. Ion Exch.* **2010**, *28*, 437−458. (b) Aneheim, E.; Ekberg, C.; Fermvik, A.; Foreman, M. R. St. J.; Grüner, B.; Hájková, Z.; Kvičalová, M. *Solvent Extr. Ion Exch.* **2011**, *29*, 157−175. (c) Wilden, A.; Schreinemachers, C.; Sypula, M.; Modolo, G. *Solvent Extr. Ion Exch.* **2011**, *29*, 190−212. (d) Magnusson, D.; Geist, A.; Wilden, A.; Modolo, G. *Solvent Extr. Ion Exch.* **2013**, *31*, 1−11. (e) Modolo, G.; Wilden, A.; Daniels, H.; Geist, A.; Magnusson, D.; Malmbeck, R. *Radiochim. Acta* **2013**, *101*, 155−162.

(12) (a) Lewis, F. W.; Harwood, L. M.; Hudson, M. J.; Drew, M. G. B.; Desreux, J. F.; Vidick, G.; Bouslimani, N.; Modolo, G.; Wilden, A.; Sypula, M.; Vu, T.-H.; Simonin, J.-P. *J. Am. Chem. Soc.* **2011**, *133*, 13093−13102. (b) Lewis, F. W.; Harwood, L. M.; Hudson, M. J.; Drew, M. G. B.; Wilden, A.; Sypula, M.; Modolo, G.; Vu, T.-H.; Simonin, J.-P.; Vidick, G.; Bouslimani, N.; Desreux, J. F. *Proc. Chem.* **2012**, *7*, 231−238.

(13) For recent molecular dynamics simulations on BTPhens and their Eu(III) complexes, see: Benay, G.; Wipff, G. *J. Phys. Chem. B* **2013**, *117*, 1110−1122.

(14) Laventine, D. M.; Afsar, A.; Hudson, M. J.; Harwood, L. M. *Heterocycles* **2012**, *86*, 1419−1429.

(15) Benay, G.; Schurhammer, R.; Wipff, G. *Phys. Chem. Chem. Phys.* **2011**, *13*, 2922−2934.

(16) (a) Cram, D. J.; Cram, J. M. *Acc. Chem. Res.* **1978**, *11*, 8−14. (b) Hancock, R. D.; Melton, D. L.; Harrington, J. M.; McDonald, F. C.; Gephart, R. T.; Boone, L. L.; Jones, S. B.; Dean, N. E.; Whitehead, J. R.; Cockrell, G. M. *Coord. Chem. Rev.* **2007**, *251*, 1678−1689.

(17) (a) Cockrell, G. M.; Zhang, G.; VanDerveer, D. G.; Thummel, R. P.; Hancock, R. D. *J. Am. Chem. Soc.* **2008**, *130*, 1420−1430. (b) Carolan, A. N.; Cockrell, G. M.; Williams, N. J.; Zhang, G.; VanDerveer, D. G.; Lee, H.-S.; Thummel, R. P.; Hancock, R. D. *Inorg. Chem.* **2013**, *52*, 15−27.

(18) Carolan, A. N.; Mroz, A. E.; El Ojaimi, M.; VanDerveer, D. G.; Thummel, R. P.; Hancock, R. D. *Inorg. Chem.* **2012**, *51*, 3007−3015.

(19) Whittaker, D. M.; Griffiths, T. L.; Helliwell, M.; Swinburne, A. N.; Natrajan, L. S.; Lewis, F. W.; Harwood, L. M.; Parry, S. A.; Sharrad, C. A. *Inorg. Chem.* **2013**, *52*, 3429−3444.

(20) Steppert, M.; Císařová, I.; Fanghänel, T.; Geist, A.; Lindqvist-Reis, P.; Panak, P.; Štěpnička, P.; Trumm, S.; Walther, C. *Inorg. Chem.* **2012**, *51*, 591−600.

(21) Hubscher-Bruder, V.; Haddaoui, J.; Bouhroum, S.; Arnaud-Neu, F. *Inorg. Chem.* **2010**, *49*, 1363−1371.

(22) For recent modelling approaches of An/Ln separations, see: (a) Petit, L.; Daul, C.; Adamo, C.; Maldivi, P. *New J. Chem.* **2007**, *31*, 1738−1745. (b) Lan, J.-H.; Shi, W.-Q.; Yuan, L.-Y.; Zhao, Y.-L.; Li, J.; Chai, Z.-F. *Inorg. Chem.* **2011**, *50*, 9230−9237. (c) Lan, J.-H.; Shi, W.-Q.; Yuan, L.-Y.; Feng, Y.-X.; Zhao, Y.-L.; Chai, Z.-F. *J. Phys. Chem. A* **2012**, *116*, 504−511. (d) Narbutt, J.; Oziminski, W. P. *Dalton Trans.* **2012**, *41*, 14416−14424.

(23) For a review, see: Lan, J.-H.; Shi, W.-Q.; Yuan, L.-Y.; Li, J.; Zhao, Y.-L.; Chai, Z.-F. *Coord. Chem. Rev.* **2012**, *256*, 1406−1417.

(24) *Materials Studio 5.5*; Accelrys Inc.: San Diego, CA.

(25) Delley, B. *J. Chem. Phys.* **2000**, *113*, 7756−7764.

(26) (a) Sun, H. *J. Phys. Chem. B* **1998**, *102*, 7338−7364. (b) McQuaid, M. J.; Sun, H.; Rigby, D. *J. Comput. Chem.* **2004**, *25*, 61−71.

(27) Geist, A.; Hill, C.; Modolo, G.; Foreman, M. R.; St, J.; Weigl, M.; Gompper, K.; Hudson, M. J.; Madic, C. *Solvent Extr. Ion Exch.* **2006**, *24*, 463−483.

(28) (a) Lewis, F. W.; Harwood, L. M.; Hudson, M. J. Patent WO2011077081A1, 2011. (b) $CyMe_4$-BTBP 1, $CyMe_4$-BTPhen 2 and precursors are produced by Technocomm, U.K. (www.technocomm.co.uk).

(29) *Methodes d'Analyses Complexométriques par les Titriplex*, 3rd ed.; E. Merck AG: Darmstadt, Germany, 1992.

(30) CrysAlis, Oxford Diffraction Ltd.: Abingdon, U.K., 2006.

(31) Sheldrick, G. M. *Acta Crystallogr.* **2008**, *A64*, 112−122.

(32) *ABSPACK*; Oxford Diffraction Ltd.: Oxford, U.K., 2005.

(33) (a) Gampp, H.; Maeder, M.; Meyer, C. J.; Zueberbuhler, A. D. *Talanta* **1985**, *32*, 95−101. (b) Gampp, H.; Maeder, M.; Meyer, C. J.; Zueberbuhler, A. D. *Talanta* **1985**, *32*, 257−264. (c) Gampp, H.; Maeder, M.; Meyer, C. J.; Zueberbuhler, A. D. *Talanta* **1985**, *32*, 1133−1139. (d) Gampp, H.; Maeder, M.; Meyer, C. J.; Zueberbuhler, A. D. *Talanta* **1986**, *33*, 943−951.

(34) From Thermometric, Experimental and Technical Note EN 014b, 2002.

(35) Hallen, D. *Pure Appl. Chem.* **1993**, *65*, 1527−1532.

(36) Ebert, K.; Ederer, H. *Computeranwendungen in der Chemie*; Wiley-VCH: Weinheim, Germany, 1985.

(37) Herbelin, A. L.; Westall, J. C. *FITEQL−A Computer Program for Determination of Chemical Equilibrium Constants from Experimental Data, version 3.2*; Report 94−01; Department of Chemistry, Oregon State University: Corvallis, OR, 1996.

(38) Dvořák, L.; Ledvinka, M.; Sobotka, M. *FAMULUS 3.1*; Computer Equipment: Prague, 1991.

(39) Lewis, F. W.; Harwood, L. M.; Hudson, M. J.; Distler, P.; John, J.; Stamberg, K.; Núñez, A.; Galán, H.; Espartero, A. G. *Eur. J. Org. Chem.* **2012**, 1509−1519.

(40) Ramachandran, G. N.; Ramakrishnan, C.; Sasisekharan, V. *J. Mol. Biol.* **1963**, *7*, 95−99.

(41) Foreman, M. R. S.; Hudson, M. J.; Drew, M. G. B.; Hill, C.; Madic, C. *Dalton Trans.* **2006**, 1645−1653.

(42) (a) Shrake, A.; Rupley, J. A. *J. Mol. Biol.* **1973**, *79*, 351−364. (b) Lee, B.; Richards, F. M. *J. Mol. Biol.* **1971**, *55*, 379−400.

(43) Bhattacharyya, A.; Gadly, T.; Mohapatra, P. K.; Ghosh, S. K.; Manna, D.; Ghanty, T. K.; Manchanda, V. K. *RSC Adv.* **2012**, *2*, 7066−7073.
(44) Seaborg, G. T. *Radiochim. Acta* **1993**, *61*, 115−122.
(45) Lewis, F. W.; Harwood, L. M.; Hudson, M. J.; Drew, M. G. B.; Modolo, G.; Sypula, M.; Desreux, J. F.; Bouslimani, N.; Vidick, G. *Dalton Trans.* **2010**, *39*, 5172−5182.
(46) See for example: (a) Comblin, V.; Gilsoul, D.; Hermann, M.; Humblet, V.; Jacques, V.; Mesbahi, M.; Sauvage, C.; Desreux, J. F. *Coord. Chem. Rev.* **1999**, *185*−*186*, 451−470. (b) Wang, P.; Saadioui, M.; Schmidt, C.; Bohmer, V.; Host, V.; Desreux, J. F.; Dozol, J. F. *Tetrahedron* **2004**, *60*, 2509−2515. (c) Desreux, J. F. *Adv. Inorg. Chem.* **2005**, *57*, 381−403. (d) Keizers, P. H. J.; Desreux, J. F.; Overhand, M.; Ubbink, M. *J. Am. Chem. Soc.* **2007**, *129*, 9292−9293. (e) Pompidor, G.; D'Aleo, A.; Vicat, J.; Toupet, L.; Giraud, N.; Kahn, R.; Maury, O. *Angew. Chem., Int. Ed.* **2008**, *47*, 3388−3391. (f) Deneil, C.; Desreux, J. F. *Chim. Nouv.* **2009**, *27*, 34−36. (g) Marcos, P. M.; Ascenso, J. R.; Segurado, M. A. P.; Bernardino, R. J.; Cragg, P. J. *Tetrahedron* **2009**, *65*, 496−503. (h) El Aroussi, B.; Dupont, N.; Bernardinelli, G.; Hamacek, J. *Inorg. Chem.* **2010**, *49*, 606−615. (i) Marcos, P. M.; Ascenso, J. R.; Segurado, M. A. P.; Cragg, P. J.; Michel, S.; Hubscher-Bruder, V.; Arnaud-Neu, F. *Supramol. Chem.* **2011**, *23*, 93−101.
(47) Lewis, F. W.; Harwood, L. M.; Hudson, M. J.; Drew, M. G. B.; Sypula, M.; Modolo, G.; Whittaker, D.; Sharrad, C. A.; Videva, V.; Hubscher-Bruder, V.; Arnaud-Neu, F. *Dalton Trans.* **2012**, *41*, 9209−9219.
(48) For a review on stability constant determination by NMR and other means, see: Thordarson, P. *Chem. Soc. Rev.* **2011**, *40*, 1305−1323.

dx.doi.org/10.1021/ic3026842 | *Inorg. Chem.* 2013, 52, 4993−5005